

B( $E2\uparrow$ ) strength in  $^{36,38}\text{Ca}$  and in mirror nuclei  $^{36}\text{S}$ ,  $^{38}\text{Ar}$ .\*

JACEK OKOŁOWICZ

Institute of Nuclear Physics, Polish Academy of Sciences, Radzikowskiego 152,  
PL-31342 Kraków, Poland

MAREK PŁOSZAJCZAK

Grand Accélérateur National d'Ions Lourds (GANIL), CEA/DSM -  
CNRS/IN2P3, BP 55027, F-14076 Caen Cedex 05, France

Recently,  $B(E2, 0_1^+ \rightarrow 2_1^+)$  transition strength have been measured in  $^{36}\text{Ca}$  and  $^{38}\text{Ca}$ . Surprisingly, the measured value in  $^{36}\text{Ca}$ :  $B(E2 \uparrow) = 131(20) e^2\text{fm}^4$ , is significantly larger than in  $^{38}\text{Ca}$ , where  $B(E2 \uparrow) = 101(11) e^2\text{fm}^4$ , whereas an opposite tendency of  $B(E2)$  values is seen in the mirror nuclei  $^{36}\text{S}$  and  $^{38}\text{Ar}$ . The resonance  $2_1^+$  in  $^{36}\text{Ca}$  lies 465 keV above the proton emission threshold and its description requires inclusion of the coupling to the continuum. In this work, we are analyzing  $B(E2 \uparrow)$  values in  $^{36}\text{Ca}$ ,  $^{36}\text{S}$ ,  $^{38}\text{Ca}$ , and  $^{38}\text{Ar}$  using the real-energy continuum shell model, the so-called shell model embedded in the continuum, in the  $(1s_{1/2} 0d_{3/2} 0f_{7/2} 1p_{3/2})$  model space with the monopole adjusted effective interaction ZBM-IO.

## 1. Introduction

$B(E2, 0_1^+ \rightarrow 2_1^+)$  transition strength provides a sensitive test of the ground state and the first  $2^+$  state wave functions in even-even nuclei. This experimental observable is also a useful indicator of the shell evolution and the variation of the nucleon-nucleon correlations. It also indicates how well the mirror symmetry is satisfied. The recent measurement of  $B(E2)$  values in  $^{36,38}\text{Ca}$  [1, 2] provided astonishingly different results as compared to the results in mirror nuclei  $^{36}\text{S}$ ,  $^{38}\text{Ar}$ .

$^{36}\text{Ca}$  has the proton shell  $Z = 20$  and the neutron subshell  $N = 16$  closed [3], whereas  $^{38}\text{Ca}$  lies in-between  $N=16$  and  $N=20$  shell closures. Indeed, the first excited state in  $^{36}\text{Ca}$  is the  $0_2^+$  state, as one might expect

---

\* Presented at the 57th Zakopane Conference on Nuclear Physics, *Extremes of the Nuclear Landscape*, Zakopane, Poland, 25 August–1 September, 2024.

in closed shell nuclei. The  $2_1^+$  state in this nucleus is one- and two-proton unbound [4]. It lies 465 keV above the one-proton emission threshold [5] and  $\sim 230$  keV above the  $0_2^+$  state [6]. It couples to the ground states of  $^{35}\text{K}$  and  $^{34}\text{Ar}$  in  $\ell = 0$  and  $\ell = 2$  partial waves, respectively. Since there is no centrifugal barrier for the one-proton (1p) decay, and the available phase space for 1p decay is significantly larger than for two-proton (2p) decay therefore, one expects that the 1p emission dominates the decay of this resonance.

The mirror nucleus  $^{36}\text{S}$  is well bound. Contrary to  $^{36}\text{Ca}$ , the first excited state is  $2_1^+$ , 6.6 MeV below the one-neutron emission threshold and  $\sim 50$  keV below the  $0_2^+$  state. This implies that the influence of continuum coupling on the structure of  $2_1^+$  states in  $^{36}\text{Ca}$  and  $^{36}\text{S}$  can be different. Indeed, the difference of  $2_1^+$  excitation energies in these nuclei is  $\sim 250$  keV, whereas the corresponding energy difference in well bound nuclei  $^{38}\text{Ca}$  and  $^{38}\text{Ar}$  is only  $\sim 50$  keV.

Coupling to the continuum may also play a role in the anomalous  $B(E2, 0_1^+ \rightarrow 2_1^+)$  transition probabilities in mirror pairs of nuclei:  $^{36}\text{Ca}$  and  $^{36}\text{S}$ , for which the  $B(E2 \uparrow)$  transition probabilities are  $131 \pm 20 e^2 \text{ fm}^4$  [1, 2] and  $89 \pm 9 e^2 \text{ fm}^4$  [5], respectively, and  $^{38}\text{Ca}$  and  $^{38}\text{Ar}$  for which experimental values are  $101 \pm 10 e^2 \text{ fm}^4$  [1, 2] and  $125 \pm 4 e^2 \text{ fm}^4$  [7], respectively. Whereas  $B(E2 \uparrow)$  in  $^{36}\text{Ca}$  is larger than in  $^{38}\text{Ca}$ , the tendency is opposite in mirror nuclei and  $B(E2 \uparrow)$  is larger in  $^{38}\text{Ar}$  than in  $^{36}\text{S}$ .

In this work, we shall apply the shell model embedded in the continuum (SMEC) [8, 9, 10], the real-energy continuum shell model, to analyze the  $B(E2, 0_1^+ \rightarrow 2_1^+)$  transition strength. The spectrum of  $^{36}\text{Ca}$  in SMEC was discussed previously in Ref. [4]. Brief presentation of SMEC and the Hamiltonian is given in Sec. 2. Discussion of results and a short summary is in Sec. 3.

## 2. Shell model embedded in the continuum

The SMEC has been extensively applied to calculate spectra and reactions for bound, weakly bound and unbound nuclear states [8, 9, 10]. Here we will present only essential features of this model and more details can be found in Refs. [8, 10].

Hilbert space in the SMEC is divided into orthogonal subspaces  $\mathcal{Q}_0, \mathcal{Q}_1, \mathcal{Q}_2, \dots$  containing 0, 1, 2,  $\dots$  particles in the scattering continuum. Since the two-proton decay provides only a tiny contribution to the total decay width of the  $2_1^+$  resonance in  $^{36}\text{Ca}$ , we shall restrict our discussion to the simplest version of SMEC with the two subspaces  $\mathcal{Q}_0, \mathcal{Q}_1$  only. An open quantum system description of  $\mathcal{Q}_0$  includes couplings to the environment of

decay channels through the energy-dependent effective Hamiltonian:

$$\mathcal{H}(E) = H_{\mathcal{Q}_0\mathcal{Q}_0} + W_{\mathcal{Q}_0\mathcal{Q}_0}(E), \quad (1)$$

where  $H_{\mathcal{Q}_0\mathcal{Q}_0}$  denotes the standard shell model (SM) Hamiltonian which describes internal dynamics, and

$$W_{\mathcal{Q}_0\mathcal{Q}_0}(E) = H_{\mathcal{Q}_0\mathcal{Q}_1} G_{\mathcal{Q}_1}^{(+)}(E) H_{\mathcal{Q}_1\mathcal{Q}_0}, \quad (2)$$

is the energy-dependent continuum coupling term, where  $E$  is the scattering energy,  $G_{\mathcal{Q}_1}^{(+)}(E)$  is the one-nucleon Green's function, and  $H_{\mathcal{Q}_0\mathcal{Q}_1}$  and  $H_{\mathcal{Q}_1\mathcal{Q}_0}$  couple the subspaces  $\mathcal{Q}_0$  with  $\mathcal{Q}_1$ . The channel state is defined by the coupling of one nucleon in the scattering continuum to the SM wave function of the nucleus  $(A-1)$ . The SMEC eigenstates  $|\Psi_\alpha^{J^\pi}\rangle$  of  $\mathcal{H}(E)$  are the linear combinations of SM eigenstates  $|\Phi_i^{J^\pi}\rangle$  of  $H_{\mathcal{Q}_0\mathcal{Q}_0}$ .

As the  $H_{\mathcal{Q}_0\mathcal{Q}_0}$  we take the ZBM-IO effective interaction which is defined in  $(1s_{1/2} 0d_{3/2} 0f_{7/2} 1p_{3/2})$  model space [11] with the two-body matrix elements of IOKIN interaction [12] and the modified  $T = 1$  cross-shell monopole terms  $\mathcal{M}(1s_{1/2} 0f_{7/2})$ ,  $\mathcal{M}(1s_{1/2} 1p_{3/2})$  which are adjusted to reproduce the low-lying states in the studied nuclei. It was argued in Ref. [1], that the ZBM2 Hamiltonian [11], defined in the same model space  $(1s_{1/2} 0d_{3/2} 0f_{7/2} 1p_{3/2})$ , provides best SM description of the  $B(E2, 0_1^+ \rightarrow 2_1^+)$  transitions probabilities in  $^{36,38}\text{Ca}$ . In the present calculation, we restrict the number of nucleon excitations from  $(1s_{1/2} 0d_{3/2})$  to  $(0f_{7/2} 1p_{3/2})$  to 2 nucleons.

For the continuum-coupling interaction we take the Wigner-Bartlett contact force:  $V_{12} = V_0 [\alpha + \beta P_{12}^\sigma] \delta(\vec{r}_1 - \vec{r}_2)$ , where  $\alpha + \beta = 1$ ,  $P_{12}^\sigma$  is the spin exchange operator, and the spin-exchange parameter takes a standard value  $\alpha = 0.73$  [8]. The radial single particle wave functions (in  $\mathcal{Q}_0$ ) and the scattering wave functions (in  $\mathcal{Q}_1$ ) are generated by the average potential which includes the central Woods-Saxon term, the spin-orbit term, and the Coulomb potential. The radius and diffuseness of the Woods-Saxon and spin-orbit potentials are  $R_0 = 1.27A^{1/3}$  fm and  $a = 0.67$  fm, respectively. The strength of the spin-orbit potential is  $V_{\text{SO}} = 6.7$  MeV for protons and 7.62 MeV for neutrons. The Coulomb part is calculated for an uniformly charged sphere with the radius  $R_0$ .

### 3. Discussion of results

Table 1 presents the continuum coupling strength  $V_0$  and the corresponding  $T = 1$  cross-shell monopoles of the ZBM-IO interaction, which allow to describe proton separation energy, excitation energy of the  $2_1^+$  state, and yield the  $B(E2 \uparrow)$  transition probabilities compatible with the data within

Table 1. The family of SMEC solutions for  $^{36}\text{Ca}$  and  $^{38}\text{Ca}$ . In the first two columns, the  $T = 1$  cross-shell monopoles (in MeV) are presented. Third column contains the continuum coupling strength  $V_0$  (in MeV fm<sup>3</sup>) which for each set of  $T = 1$  cross-shell monopoles in the first two columns is adjusted to reproduce the proton separation energy and energy of the  $2_1^+$  state. Next columns contain the following sequence:  $B(E2 \uparrow)$  values (in units of  $e^2\text{fm}^4$ ), and the ground state fractions  $F_p(0)$ ,  $F_p(2)$ ,  $F_n(0)$  and  $F_n(2)$  of proton/neutron parts excited from  $(1s_{1/2}0d_{3/2})$  to  $(0f_{7/2}1p_{3/2})$  shells.  $B(E2 \uparrow)$  values in this table have been calculated with the effective charges:  $e_p = 1.236$ ,  $e_n = 0.409$ .

$\mathcal{M}$		$^{36}\text{Ca}$					
$sf_{7/2}$	$sp_{3/2}$	$V_0$	$B(E2 \uparrow)$	$F_n(0)$	$F_n(2)$	$F_p(0)$	$F_p(2)$
-2.078	-2.657	0	110	0.977	0.003	0.659	0.322
-2.137	-2.554	-61.3	116.7	0.978	0.003	0.635	0.346
-2.177	-2.477	-85	121	0.979	0.003	0.616	0.366
-2.227	-2.377	-113	126	0.980	0.003	0.588	0.395
-2.277	-2.247	-139	129	0.981	0.003	0.557	0.427
$\mathcal{M}$		$^{38}\text{Ca}$					
$sf_{7/2}$	$sp_{3/2}$	$V_0$	$B(E2 \uparrow)$	$F_n(0)$	$F_n(2)$	$F_p(0)$	$F_p(2)$
-2.078	-2.657	0	66.9	0.870	0.045	0.613	0.303
-2.137	-2.554	-61.3	82.5	0.873	0.045	0.580	0.337
-2.177	-2.477	-85	93.4	0.874	0.044	0.554	0.364
-2.227	-2.377	-113	108	0.877	0.042	0.519	0.400
-2.277	-2.247	-139	121	0.881	0.040	0.482	0.440

the experimental uncertainties for  $^{36}\text{Ca}$  and  $^{38}\text{Ca}$  simultaneously. One can see that the monopoles:  $\mathcal{M}^{T=1}(1s_{1/2}1p_{3/2})$  and  $\mathcal{M}^{T=1}(1s_{1/2}0f_{7/2})$ , are anti-correlated and that the demanded criteria are satisfied by the whole family of solutions.

Table 1 shows also the fractions  $F_n(0)$ ,  $F_n(2)$ ,  $F_p(0)$  and  $F_p(2)$  of the proton and neutron parts in the ground state wave function which are excited from  $(1s_{1/2}0d_{3/2})$  to  $(0f_{7/2}1p_{3/2})$ . The sum:  $F_{n/p}(0)+F_{n/p}(2)+F_{np}(11)$ , where  $F_{np}(11)$  is the fraction corresponding to the simultaneous excitation of one proton and one neutron from  $(1s_{1/2}0d_{3/2})$  to  $(0f_{7/2}1p_{3/2})$ , is normalized to 1. One may notice that the fraction  $F_p(0)$  depends strongly on the monopoles  $\mathcal{M}^{T=1}(1s_{1/2}1p_{3/2})$ ,  $\mathcal{M}^{T=1}(1s_{1/2}0f_{7/2})$ , and the continuum-coupling strength  $V_0$ , whereas  $F_{np}(11)$  remains practically constant. Changes of  $F_n(0)$  in the whole range of parameters are small. Moreover,  $F_n(0)$  and  $F_p(0)$  in  $^{38}\text{Ca}$  are significantly smaller than in  $^{36}\text{Ca}$ .

Table 2 contains information on the family of monopole terms  $\mathcal{M}^{T=1}(1s_{1/2}1p_{3/2})$ ,

Table 2. The family of SMEC solutions for mirror nuclei:  $^{36}\text{S}$  and  $^{38}\text{Ar}$ . For details see the caption of Table 1.

$\mathcal{M}$				$^{36}\text{S}$			
$sf_{7/2}$	$sp_{3/2}$	$V_0$	$B(E2 \uparrow)$	$F_n(0)$	$F_n(2)$	$F_p(0)$	$F_p(2)$
-2.112	-1	0	89.0	0.697	0.288	0.982	0.003
-2.167	-0.077	-83	75.8	0.670	0.318	0.984	0.003
-2.183	0.423	-96	71.7	0.662	0.326	0.985	0.003
-2.194	0.923	-105.3	68.5	0.655	0.333	0.985	0.003
-2.207	1.923	-116	64.7	0.648	0.341	0.986	0.003
$\mathcal{M}$				$^{38}\text{Ar}$			
$sf_{7/2}$	$sp_{3/2}$	$V_0$	$B(E2 \uparrow)$	$F_n(0)$	$F_n(2)$	$F_p(0)$	$F_p(2)$
-2.112	-1	0	126.4	0.601	0.324	0.883	0.043
-2.167	-0.077	-83	126.4	0.559	0.368	0.886	0.042
-2.183	0.423	-96	125.0	0.546	0.382	0.887	0.041
-2.194	0.923	-105.3	125.9	0.536	0.393	0.888	0.041
-2.207	1.923	-116	125.6	0.522	0.407	0.889	0.040

$\mathcal{M}^{T=1}(1s_{1/2}0f_{7/2})$ , and the continuum-coupling strength  $V_0$ , which allow to reproduce the neutron separation energy, excitation energy of the  $2_1^+$  state, and provide the  $B(E2 \uparrow)$  values which are compatible with the experimental data in  $^{36}\text{S}$  and  $^{38}\text{Ar}$ . Changes of the  $\mathcal{M}^{T=1}(1s_{1/2},0f_{7/2})$  monopole are small, while those of  $\mathcal{M}^{T=1}(1s_{1/2},1p_{3/2})$  are large and different from the corresponding monopole in  $^{36}\text{Ca}$  and  $^{38}\text{Ca}$ . Range of  $F_p(0)$  variation in  $^{36}\text{Ca}$  ( $^{38}\text{Ca}$ ) is significantly larger than the corresponding variations of  $F_n(0)$  in the mirror nuclei  $^{36}\text{S}$  ( $^{38}\text{Ar}$ ). It is important to notice that  $B(E2 \uparrow)$  for  $^{38}\text{Ar}$  is almost constant in a large interval of parameters  $\mathcal{M}^{T=1}(1s_{1/2}1p_{3/2})$  and  $V_0$ . This property has been used to tune the effective charges for all considered nuclei:  $^{36}\text{Ca}$ ,  $^{36}\text{S}$ ,  $^{38}\text{Ca}$ , and  $^{38}\text{Ar}$ .

Dependence of the  $B(E2, 0_1^+ \rightarrow 2_1^+)$  transitions probabilities on the continuum coupling strength  $V_0$  is shown in Fig. 1 for mirror pairs of nuclei ( $^{36}\text{Ca}$ ,  $^{36}\text{S}$ ), and ( $^{38}\text{Ca}$ ,  $^{38}\text{Ar}$ ). The cross-shell monopoles in ZBM-IO interaction are kept constant as a function of  $V_0$ . Horizontal lines show the experimental uncertainties of  $B(E2 \uparrow)$ . For more information, see the caption of Fig. 1. One may notice a weak dependence on  $V_0$  in  $^{36}\text{Ca}$ . Even weaker dependence is seen in  $^{38}\text{Ca}$ , and almost no dependence on the strength of the continuum coupling is in  $^{38}\text{Ar}$ . The  $B(E2 \uparrow)$  curves shown in this figure have been obtained for the effective charges equal:  $e_p = 1.236$ ,  $e_n = 0.409$ .

Dependence of the ground state energy of  $^{36}\text{Ca}$ ,  $^{38}\text{Ca}$ ,  $^{36}\text{S}$  and  $^{38}\text{Ar}$

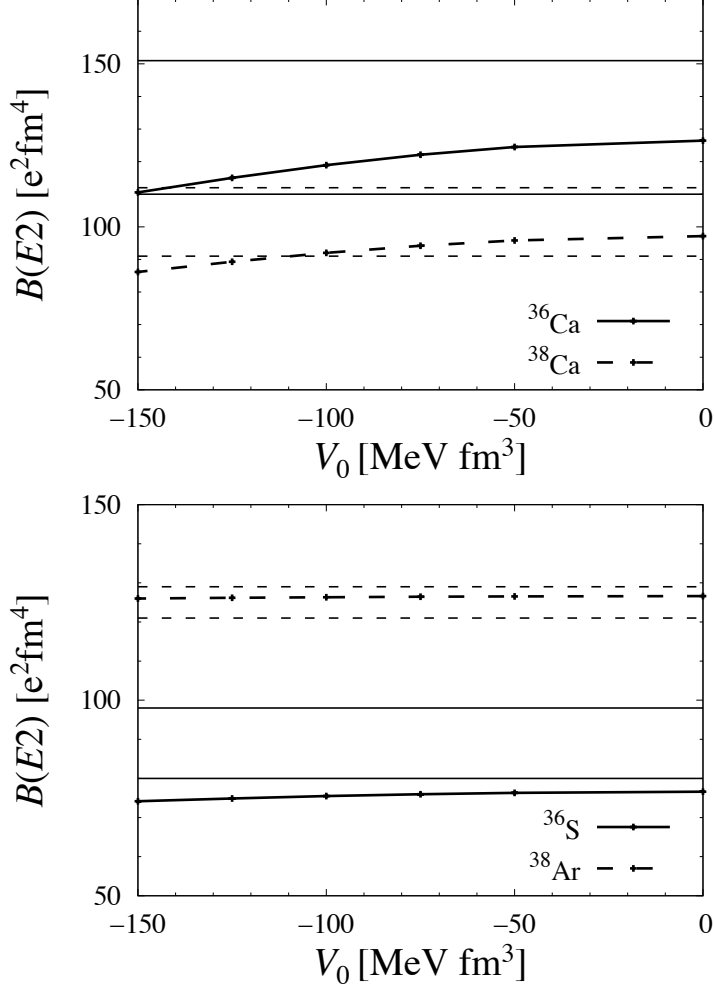


Fig. 1. Upper panel: The  $B(E2 \uparrow)$  transition probabilities in  $^{36}\text{Ca}$  (the solid line) and  $^{38}\text{Ca}$  (the long-dashed line), calculated in SMEC, are plotted as a function of the continuum coupling strength  $V_0$ . Horizontal solid and short-dashed lines show the uncertainties of the experimental  $B(E2 \uparrow)$  values in  $^{36}\text{Ca}$  and  $^{38}\text{Ca}$ , respectively. The  $T = 1$  cross-shell monopoles of ZBM-IO interaction in this panel are:  $\mathcal{M}^{T=1}(1s_{1/2} 1p_{3/2}) = -2.477$  MeV and  $\mathcal{M}^{T=1}(1s_{1/2} 0f_{7/2}) = -2.177$  MeV. Lower panel: The same as in the upper panel but for the mirror nuclei  $^{36}\text{S}$  and  $^{38}\text{Ar}$ . The  $T = 1$  cross-shell monopoles in this case are:  $\mathcal{M}^{T=1}(1s_{1/2} 1p_{3/2}) = -0.077$  MeV and  $\mathcal{M}^{T=1}(1s_{1/2} 0f_{7/2}) = -2.177$  MeV.

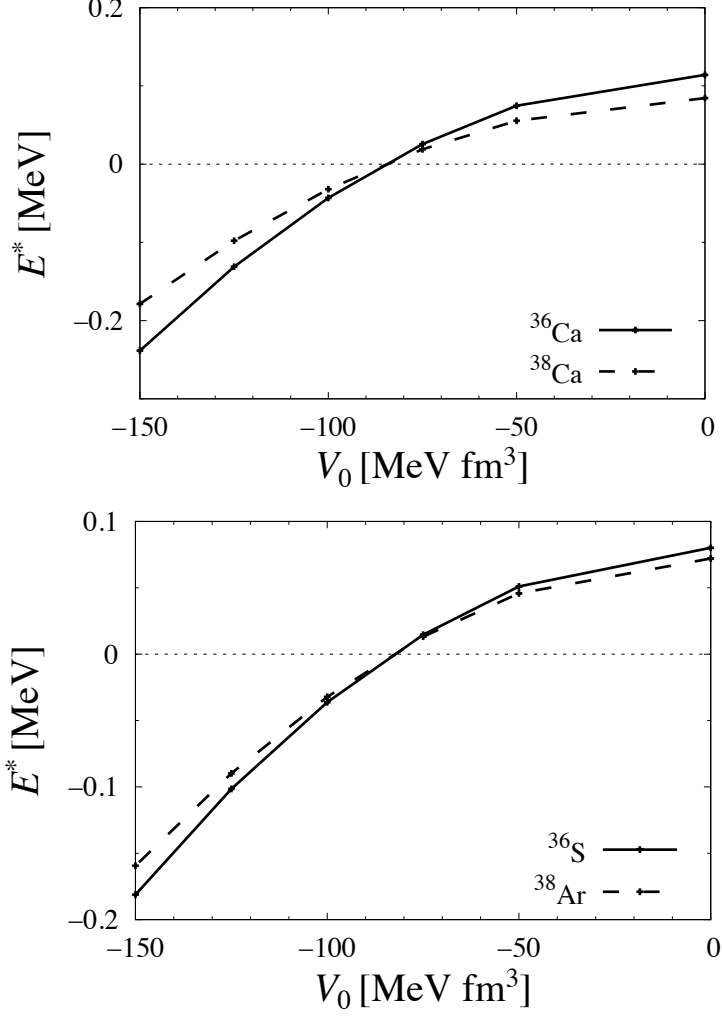


Fig.2. Upper panel: Ground state energy of  $^{36}\text{Ca}$  and  $^{38}\text{Ca}$  is plotted as a function of the continuum coupling strength  $V_0$  for fixed values of  $T = 1$  cross-shell monopoles:  $\mathcal{M}^{T=1}(1s_{1/2} 1p_{3/2}) = -2.477$  MeV and  $\mathcal{M}^{T=1}(1s_{1/2} 0f_{7/2}) = -2.177$  MeV. The dashed horizontal line corresponds to the situation when the ground state  $0_1^+$  is at the experimental distance from the state  $2_1^+$ . Lower panel: The same as in the upper panel but for mirror nuclei  $^{36}\text{S}$  and  $^{38}\text{Ar}$ . The  $T = 1$  cross-shell monopoles in this case are:  $\mathcal{M}^{T=1}(1s_{1/2} 1p_{3/2}) = -0.077$  MeV and  $\mathcal{M}^{T=1}(1s_{1/2} 0f_{7/2}) = -2.177$  MeV.

on the continuum-coupling strength parameter  $V_0$  is shown in Fig. 2. One

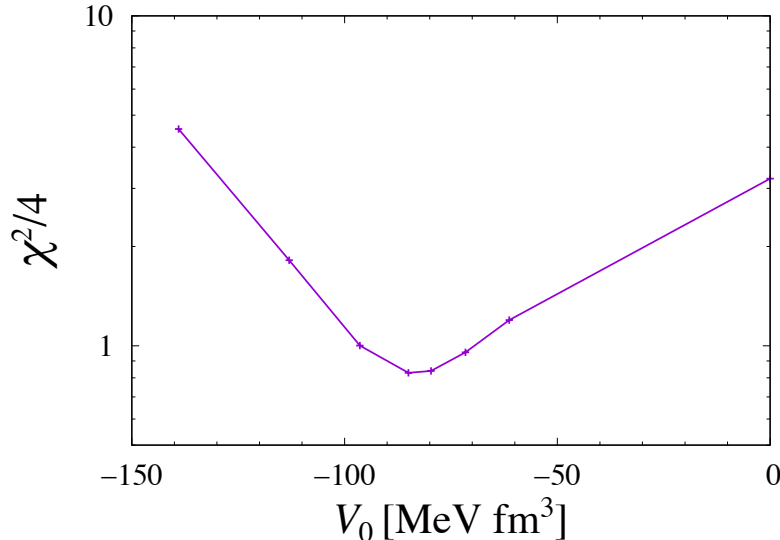


Fig. 3. Function  $\chi^2$  for calculated  $B(E2 \uparrow)$  values in  $^{36}\text{Ca}$ ,  $^{38}\text{Ca}$ ,  $^{36}\text{S}$  and  $^{38}\text{Ar}$  (see Tables 1 and 2) is plotted as a function of the continuum coupling strength  $V_0$  and normalized to the number of data. At the minimum, value of the  $\chi^2$  function is:  $\chi^2/4 = 0.82$ .

can see that this dependence is rather weak for all considered nuclei. The strongest effect is seen in the ground state of  $^{36}\text{Ca}$ . The change of an excitation energy of the  $2_1^+$  state is mainly due to the down-sloping of the ground state energy in all considered nuclei.

Using the calculated  $B(E2 \uparrow)$  values for different continuum-coupling strengths  $V_0$  (see the Tables 1 and 2), one can search for optimal parameters of the ZBM-IO interaction which reproduce best the experimental  $B(E2 \uparrow)$  values. Figure 3 presents the function  $\chi^2$  normalized to the number of data points which is plotted as a function of  $V_0$  for all  $B(E2 \uparrow)$  values. We can see that the preferable continuum coupling strength is  $V_0 \approx -85 \text{ MeV fm}^3$ .

SMEC results corresponding to the minimum of  $\chi^2$  function (see Fig. 3) are presented in Table 3. The optimal monopole  $\mathcal{M}^{T=1}(1s_{1/2}, 0f_{7/2}) \simeq -2.17 \text{ MeV}$  is almost the same in mirror pairs ( $^{36}\text{Ca}/^{36}\text{S}$ ) and ( $^{38}\text{Ca}/^{38}\text{Ar}$ ). On the other hand, the optimal monopole  $\mathcal{M}^{T=1}(1s_{1/2}, 1p_{3/2})$  changes strongly going from  $^{36,38}\text{Ca}$  to their mirror partners  $^{36}\text{S}, ^{38}\text{Ar}$ . The optimal continuum-coupling strength is almost the same in  $^{36,38}\text{Ca}$ ,  $^{36}\text{S}$ ,  $^{38}\text{Ar}$  and equals  $V_0 \simeq -83 \text{ MeV fm}^3$ .

In Table 4 we have collected  $F_q$  values for the most favorable monopole



Table 3. Results of the  $\chi^2$  analysis of  $B(E2 \uparrow)(V_0)$  (see Fig. 3 and Tables 1, 2) for  $^{36}\text{Ca}$ ,  $^{38}\text{Ca}$ ,  $^{36}\text{S}$  and  $^{38}\text{Ar}$ . Theoretical errors are due to experimental uncertainties of the separation energies [13].  $B(E2 \uparrow)$  are given in units  $e^2\text{fm}^4$ , monopole terms are in MeV, and  $V_0$  is given in units  $\text{MeV fm}^3$ . The effective charges are:  $e_p = 1.236$ ,  $e_n = 0.409$ . Experimental  $B(E2 \uparrow)$  values for  $^{36,38}\text{Ca}$  are taken from Ref. [1] and for  $^{36}\text{S}$ ,  $^{38}\text{Ar}$  from Ref. [7]

	$^{36}\text{Ca}$	$^{38}\text{Ca}$	$^{36}\text{S}$	$^{38}\text{Ar}$
$1s_{1/2} 0f_{7/2}$		-2.177		-2.167
$1s_{1/2} 1p_{3/2}$		-2.477		-0.077
$V_0$	$-85_{-14}^{+17}$	$-85.16_{-0.12}^{+0.11}$	$-82.98 \pm 0.10$	$-83.01 \pm 0.12$
$B(E2 \uparrow)$	$120.9_{-1.8}^{+1.9}$	$93.375 \pm 0.01$	$75.826 \pm 0.002$	$126.4190 \pm 0.0005$
exp.:	$131 \pm 20$	$101 \pm 11$	$89 \pm 9$	$125 \pm 4$

Table 4.  $F_n(0)$ ,  $F_n(2)$ ,  $F_p(0)$  and  $F_p(2)$  for  $0_1^+$  and  $2_1^+$  states in all considered nuclei for the most favorable monopole modifications (*cf* Table 3).

Nucleus	$J^\pi$	$F_p(0)$	$F_p(2)$	$F_n(0)$	$F_n(2)$
$^{36}\text{Ca}$	$0^+$	0.6157	0.3664	0.9792	0.0029
	$2^+$	0.1295	0.8588	0.9880	0.0003
$^{38}\text{Ca}$	$0^+$	0.5542	0.3639	0.8744	0.0436
	$2^+$	0.3413	0.5770	0.9117	0.0066
$^{36}\text{S}$	$0^+$	0.9842	0.0030	0.6695	0.3177
	$2^+$	0.9829	0.0005	0.2575	0.7259
$^{38}\text{Ar}$	$0^+$	0.8858	0.0415	0.5591	0.3683
	$2^+$	0.9223	0.0055	0.3202	0.6076

modification (see Table 3) in  $^{36,38}\text{Ca}$ ,  $^{36}\text{S}$ , and  $^{38}\text{Ar}$ . For the ground state  $0_1^+$  in  $^{36}\text{Ca}$ , fraction of the  $F_p(0)$  part excited from  $(1s_{1/2}0d_{3/2})$  to  $(0f_{7/2}1p_{3/2})$  is close to the fraction  $F_n(0)$  in the mirror nucleus  $^{36}\text{S}$ , also the fractions  $F_n(0)$  in  $^{36}\text{Ca}$  and  $F_p(0)$  in  $^{36}\text{S}$  are nearly identical. In  $^{38}\text{Ca}$ , fraction of the proton part  $F_p(0)$  is almost identical with the fraction of the neutron part  $F_n(0)$  in  $^{38}\text{Ar}$ . Similarly the fraction  $F_n(0)$  in  $^{38}\text{Ca}$  is practically identical with the  $F_p(0)$  fraction in  $^{38}\text{Ar}$ . Therefore, one may conclude that whereas the mirror symmetry in the ground state of nuclei  $^{36}\text{Ca}$  and  $^{36}\text{S}$  is only slightly broken, so it is satisfied in  $^{38}\text{Ca}$  and  $^{38}\text{Ar}$ .

A different situation is seen in the  $2_1^+$  state. The fraction of neutrons excited from  $(1s_{1/2}0d_{3/2})$  to  $(0f_{7/2}1p_{3/2})$  in  $^{36}\text{S}$  is significantly smaller than

the corresponding fraction of the proton part in  $^{36}\text{Ca}$ . This striking difference in the occupation of  $0f_{7/2}1p_{3/2}$  shells has also its counterpart in the reverse order of  $2_1^+$  and  $0_2^+$  states in  $^{36}\text{Ca}$  as compared with  $^{36}\text{S}$  [6]. In  $^{38}\text{Ca}$ ,  $^{38}\text{Ar}$ , on the contrary, the mirror symmetry in  $2_1^+$  states is well preserved.

Additional information about the structure of mirror pairs of nuclei:  $^{36}\text{Ca}$ ,  $^{36}\text{S}$  and  $^{38}\text{Ca}$ ,  $^{38}\text{Ar}$ , is provided by the spectroscopic factors presented in Table 5. One may notice that spectroscopic factors in the ground states of all considered nuclei are significantly larger than in the excited states  $2_1^+$  and  $0_2^+$ . In particular,  $C^2\mathcal{S}_{s_{1/2}}(0_2^+)$  and  $C^2\mathcal{S}_{s_{1/2}}(2_1^+)$  are smaller by one and three orders of magnitude, respectively, than the ground state spectroscopic factor  $C^2\mathcal{S}_{s_{1/2}}(0_1^+)$ . Moreover, the spectroscopic factor  $C^2\mathcal{S}_{s_{1/2}}(0_1^+)$  in  $^{36}\text{Ca}$ ,  $^{36}\text{S}$  is larger than the corresponding spectroscopic factor in  $^{38}\text{Ca}$ ,  $^{38}\text{Ar}$ .

Table 5. SMEC spectroscopic factors for  $0_1^+$ ,  $0_2^+$ ,  $2_1^+$  states in  $^{36}\text{Ca}$ ,  $^{38}\text{Ca}$ ,  $^{36}\text{S}$  and  $^{38}\text{Ar}$ .  $C^2\mathcal{S}_{\ell_j}(J_i^\pi)$  denote proton (neutron) spectroscopic factors in  $^{36,38}\text{Ca}$  ( $^{36}\text{S}$ ,  $^{38}\text{Ar}$ ).

Nucleus	$C^2\mathcal{S}_{s_{1/2}}(0_1^+)$	$C^2\mathcal{S}_{s_{1/2}}(0_2^+)$	$C^2\mathcal{S}_{d_{3/2}}(2_1^+)$	$C^2\mathcal{S}_{s_{1/2}}(2_1^+)$
$^{36}\text{Ca}$	2.903	0.534	0.0030	0.0054
$^{38}\text{Ca}$	2.320	0.586	0.0408	0.0078
$^{36}\text{S}$	3.019	0.470	0.0004	0.0070
$^{38}\text{Ar}$	2.300	0.611	0.0368	0.0080

Finally two observations are common. First, the excitation energy of  $2_1^+$  always increases with increasing the continuum coupling strength even though this state couples only weakly to the continuum due to a very small spectroscopic factor  $C^2\mathcal{S}_{s_{1/2}}(2_1^+)$ . This is due to a much stronger influence of the coupling to the continuum on the ground states, even though these states are well bound. Secondly,  $B(E2 \uparrow)$  always decreases with increasing continuum coupling strength for any combinations of monopole changes.

The mirror symmetry in the pair of nuclei  $^{38}\text{Ca}$  and  $^{38}\text{Ar}$  is well satisfied as the spectroscopic factors are almost identical (see Table 5), and the difference of ground state energies as well as the difference of  $2_1^+$  energies in these nuclei is very small.

On the contrary, the mirror symmetry in  $^{36}\text{Ca}$  and  $^{36}\text{S}$  is strongly violated. The spectroscopic factors  $C^2\mathcal{S}_{s_{1/2}}(0_1^+)$ ,  $C^2\mathcal{S}_{s_{1/2}}(0_2^+)$  in this pair of nuclei are different. Moreover, the order of  $2_1^+$  and  $0_2^+$  states is different in  $^{36}\text{Ca}$  and in  $^{36}\text{S}$ . This effect can be traced back partially to the proximity of the proton decay threshold in  $^{36}\text{Ca}$  and to the larger spectroscopic factor  $C^2\mathcal{S}_{s_{1/2}}(0_2^+)$  in  $^{36}\text{Ca}$  than in  $^{36}\text{S}$ .

In conclusion, anomalous values of  $B(E2, 0_1^+ \rightarrow 2_1^+)$  transition probability in  $^{36}\text{Ca}$  and  $^{38}\text{Ca}$  as compared with the values in the mirror nuclei  $^{36}\text{S}$  and  $^{38}\text{Ar}$ , revealed strong mirror symmetry breaking in the pair  $^{36}\text{Ca}$  and  $^{36}\text{S}$ . The SMEC provides good description of all four  $B(E2, 0_1^+ \rightarrow 2_1^+)$  transition probabilities using the ZBM-IO interaction with a monopole term  $\mathcal{M}^{T=1}(1s_{1/2}, 1p_{3/2})$  which is modified when going from  $^{36,38}\text{Ca}$  to  $^{36}\text{S}$ ,  $^{38}\text{Ar}$ .

The most important difference is seen in the structure of  $2_1^+$  state in  $^{36}\text{Ca}$  and  $^{36}\text{S}$ . The fraction  $F_p(2)$  of proton part excited from  $(1s_{1/2}0d_{3/2})$  to  $(0f_{7/2}1p_{3/2})$  in the proton unbound  $2_1^+$  state of  $^{36}\text{Ca}$  is considerably larger than the corresponding neutron part  $F_n(2)$  in  $^{36}\text{S}$ . In general, main effects of the continuum coupling in studied nuclei are concentrated in the ground state  $0_1^+$  and to a smaller extent in the excited  $0_2^+$  state. The reverse order of the  $2_1^+$  and  $0_2^+$  states in  $^{36}\text{Ca}$  is the combined effect of the proximity of  $0_2^+$  resonance to the particle emission threshold and the spectroscopic factor  $\mathcal{C}^2\mathcal{S}_{s_{1/2}}(0_2^+)$  which is two-orders of magnitude bigger than the  $\mathcal{C}^2\mathcal{S}_{s_{1/2}}(2_1^+)$ .

*Acknowledgements*– We wish to thank Witek Nazarewicz and Simin Wang for a useful discussion.

## REFERENCES

- [1] N. Dronchi, D. Weisshaar, B. A. Brown, A. Gade, R. J. Charity, L. G. Sobotka, K. W. Brown, W. Reviol, D. Bazin, P. J. Farris, A. M. Hill, J. Li, B. Longfellow, D. Rhodes, S. N. Paneru, S. A. Gillespie, A. Anthony, E. Rubino, and S. Biswas. Measurement of the  $b(e2 \uparrow)$  strengths of  $^{36}\text{Ca}$  and  $^{38}\text{Ca}$ . *Phys. Rev. C*, 107:034306, Mar 2023.
- [2] T. Beck, A. Gade, B. A. Brown, J. A. Tostevin, D. Weisshaar, D. Bazin, K. W. Brown, R. J. Charity, P. J. Farris, S. A. Gillespie, A. M. Hill, J. Li, B. Longfellow, W. Reviol, and D. Rhodes. Probing proton cross-shell excitations through the two-neutron removal from  $^{38}\text{Ca}$ . *Phys. Rev. C*, 108:L061301, Dec 2023.
- [3] C. R. Hoffman, T. Baumann, D. Bazin, J. Brown, G. Christian, P. A. DeYoung, J. E. Finck, N. Frank, J. Hinnefeld, R. Howes, P. Mears, E. Mosby, S. Mosby, J. Reith, B. Rizzo, W. F. Rogers, G. Peaslee, W. A. Peters, A. Schiller, M. J. Scott, S. L. Tabor, M. Thoennessen, P. J. Voss, and T. Williams. Determination of the  $n = 16$  shell closure at the oxygen drip line. *Phys. Rev. Lett.*, 100:152502, Apr 2008.
- [4] J. Okolowicz, M. Ploszajczak, and Yan an Luo. Continuum coupling effects in spectra of mirror nuclei and binding systematics. *Acta Physica Polonica B*, 39:389–400, 2007.
- [5] A. Buerger, F. Azaiez, Z. Dombradi, A. Alogra, B. Bastin, G. Benzoni, A. Al-Kahtib, E. Clement, Z Dlouhy, A. Gorgen, S. Grevy, W. Korten, Geirr Sletten,

- C. Timis, D. Verney, and S. Williams. Spectroscopy around  $36\text{Ca}$ . *Acta Physica Polonica B*, 38(4):1353–1357, 2007.
- [6] L. Lalanne, O. Sorlin, A. Poves, M. Assié, F. Hammache, S. Koyama, D. Suzuki, F. Flavigny, V. Girard-Alcindor, A. Lemasson, A. Matta, T. Roger, D. Beaumel, Y. Blumenfeld, B. A. Brown, F. De Oliveira Santos, F. Delaunay, N. de Séréville, S. Franchoo, J. Gibelin, J. Guillot, O. Kamalou, N. Kitamura, V. Lapoux, B. Mauss, P. Morfouace, M. Niikura, J. Pancin, T. Y. Saito, C. Stodel, and J-C. Thomas. Structure of  $^{36}\text{Ca}$  under the coulomb magnifying glass. *Phys. Rev. Lett.*, 129:122501, Sep 2022.
- [7] B. Pritychenko, M. Birch, and B. Singh. Revisiting grodzins systematics of  $b(e2)$  values. *Nuclear Physics A*, 962:73–102, 2017.
- [8] J. Okołowicz, M. Płoszajczak, and I. Rotter. Dynamics of quantum systems embedded in a continuum. *Phys. Rep.*, 374(4):271 – 383, 2003.
- [9] K. Bennaceur, F. Nowacki, J. Okołowicz, and M. Płoszajczak. *Nucl. Phys. A*, 671:203, 2000.
- [10] J. Rotureau, J. Okołowicz, and M. Płoszajczak. *Nucl. Phys. A*, 767:13, 2006.
- [11] E Caurier, K Langanke, G Martínez-Pinedo, F Nowacki, and P Vogel. Shell model description of isotope shifts in calcium. *Physics Letters B*, 522(3):240–244, 2001.
- [12] S. Nummela, P. Baumann, E. Caurier, P. Dessagne, A. Jokinen, A. Knipper, G. Le Scornet, C. Miché, F. Nowacki, M. Oinonen, Z. Radivojevic, M. Ramdhane, G. Walter, and J. Äystö. Spectroscopy of  $^{34,35}\text{Si}$  by  $\beta$  decay:  $sd - fp$  shell gap and single-particle states. *Phys. Rev. C*, 63:044316, Mar 2001.
- [13] <http://www.nndc.bnl.gov/ensdf>, 2015.